EasyChair Preprint

№ 10245

Performance Characterization of EEEC (Eolic Energy Unit) for Horizontal Axis Wind Turbine

Abdul Basit, Ali Sarosh, Osama Ali Ahmed Awan,
Hassan Shuaib and Abdur Rehman Khan

May 23, 2023

Performance Characterization of EEEC (Eolic Energy Unit) for Horizontal Axis Wind Turbine

Abdul Basit[a] abdulbasitawan16@gmail.com
Ali Sarosh[b] ali.sarosh@mail.au.edu.pk
Osama Ali Ahmed Awan[c] osamaaliahmadwan@outlook.com
Hassan Shuaib[d] hassanshuaibabbasi@gmail.com
Abdur Rehman Khan[e] khanabdurrehman101@gmail.com

[abcde]*Department of Mechanical and Aerospace engineering*
Air University
Islamabad, Pakistan.

***Abstract*— Wind energy is one of the fastest-growing forms of renewable energy which can be extracted using a wind turbines such as the Horizontal Axis Wind Turbines (HAWTs). All HAWT systems must go through experimental characterization for performance assessments. For this purpose, highly specialized wind units are employed. In this research a testing procedure has been evolved for characterizing the various HAWT configurations under variable operating conditions by using the Eolic Energy Units (EEEC). This research aims at developing comparative performance characterization curves for the EEEC unit by using the design of experiment (DoE) approach applied to HAWT system. The experiments for characterization have been conducted under different load and no-load conditions. The input parameters that include blade angles, the number of blades, and wind speeds have also been varied. Moreover, the results have been verified and validated through analytical calculations by using the Blade Element and Momentum (BEM) theory and computational analysis on ANSYS CFX. Substantial number of performance characteristic curves have been developed with good conformance of results**.

Keywords*— *Eolic energy unit (EEEC), Horizontal Axis Wind Turbine (HAWT), Experimental Analysis, Load conditions, Design of Experiment (DoE), CFX, BEM

TOPICS COVERED IN THE PAPER

I. INTRODUCTION

As the world is facing multiple challenges such as climate change, which is raising the chance of floods, famines, etc. Understanding the situation, 195 countries signed an agreement in which they agreed to work for sustainable and prosperous world . Subsequently, the United Nations Organization has defined 17 sustainable development goals, which are interconnected with each other, for the sustainability of the Earth. However, the achievement of UN SDGs 7 and 13 mainly depends on producing clean and efficient energy to meet the world's requirements [1]. As the non-renewable energy resources add harmful emissions to the environment. Therefore, the world is currently transitioning the energy sector to depend solely on renewable and sustainable energy resources. There are many sources of renewable energy that include wind, solar, hydro, geothermal energy, etc. These energy resources have the potential to overcome the harmful effects of fossil fuels. Of these renewable energies, wind energy has substantial potential to meet a major part of the world's energy requirements. Wind energy is expected to meet almost 35 percent of the world's energy requirements by the year 2050 [2]. There are many advantages of using wind energy such as the production of eco-friendly and cheaper power.

The machines which extract wind energy from wind are known as wind turbines. There are many types of wind turbines such as VAWTs, HAWTs, CAWTs, et cetera that are used for extracting energy from wind. VAWTs are generally used for small-scale energy production, whereas HAWTs are one of the most efficient wind turbines for large-scale energy production. This is because HAWTs are more efficient, and they have more power coefficient with Betz's limit of 0.59 as compared to VAWT which has 0.34. Despite having great potential for power production, most of the HAWTs are unable to extract the expected 59.6% of energy from the wind because of the losses incurred.

Rahul et al. [3] have performed experiments on a scaled version of the 3kW HAWT to analyze different parameters like tip speed ratio, torque, and power performance. Analytical calculations have been done using BEM theory while the computational part has been done on ANSYS Fluent. Hsiao et al. [4] have performed experiments on HAWT with three different blade shapes. Experimental results have shown that both OPT and UOT have the same coefficient of performance of 0.428 at different tip speed ratios. Eswaran et al. [5] have performed CFD analysis on HAWT. CFD results have shown that power comes out to be maximum at 90° blade angle, which is 2.2 MW. Chi-Jeng & Wang [6] have analyzed aerodynamic performance of HAWT blades using analytical techniques. Results have shown that modified BEM theory is more accurate as compared to others.

To evaluate and design efficient HAWTs. An Eolic Energy Unit (EEEC) [7] has recently been commissioned at the IC Engine and Power Plant Lab of DMAE (IAA), Air University Islamabad. EEEC is an apparatus of EDIBON for analyzing the conversion of the kinetic energy of wind into electrical energy. It is a computer-controlled apparatus that can also be used to study the effects of different input parameters like wind speed, blade angle, etc. on turbine performance.

Design of Experiment [8] is the systematic technique used to conduct, analyze, and interpret experiments to analyze the effect of different parameters on output. DOE is classified into two types: one is deterministic, and the other is a stochastic model. In a deterministic model, the output of a system is calculated without any randomness. All the data necessary for the prediction of output is available; there is no need to predict any input. On the other hand, stochastic model possesses some randomness. As in this work, there is no randomness; all the required input variables needed to predict output are available, so this research follows the deterministic model.

Problem statement: This research is used for characterization and performance of Eolic Energy Unit under specific conditions, three different parameters have been selected which include blade angle, wind speed, and the number of blades with different load conditions.

Blade angle and number of blades are put on right side of design of experiment because their variations are the most difficult one and time taking while wind speed is on most right side because its variations is easily changeable. The characterization curves for EEEC unit present at IC and Power Plant lab, Air University, have been developed. Experiments have been performed on different load conditions. Analytical and computational analyses have also been performed to establish the veracity of experimental results. Analytical calculations have been done by using Blade Element and Momentum (BEM) theory. Furthermore, for validation of experimental test results, computational analysis has been done on HAWT using ANSYS CFX for the case of turbulent flows. The qualitative and quantitative results of characteristic curves of EEEC unit are verifiable through alternate analysis. All the results have been verified and validated.

II. DESIGN OF EXPERIMENT AND EOLIC ENERGY UNIT

A. *Methodology*

First, DOE is established, then experimentations are performed on the basis of DOE. The results of experiments have been verified and validated through analytical calculations by using the Blade Element and Momentum (BEM) theory and computational analysis on ANSYS CFX.

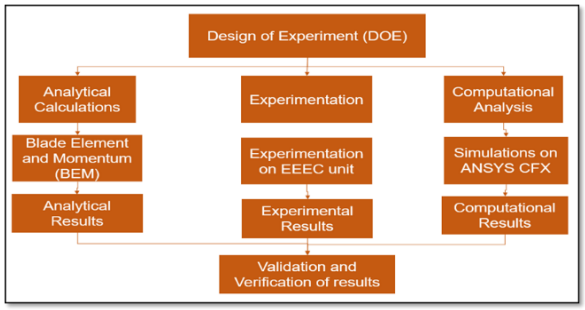

Fig. 1. Flow Chart for Methodology

B. *Experimental Test Unit*

To generate the characteristic curves of the test unit, wind tunnel experiments have been performed on EEEC at IC Engine and power plant lab, Air University. EEEC unit consists of an aerogenerator which is used for the analysis of wind turbines. The EEEC unit is a scale-designed laboratory designed to study the effect of different parameters on the performance of wind turbines. The EEEC unit consists of a fan, rotor with six blades, anemometer, speed sensor, voltage probe (Wattmeter), current probe (Wattmeter), load module, temperature sensor, J-type thermocouple, and a regulator and control system (SCADA). Fig. 2 shows the complete EEEC unit setup.

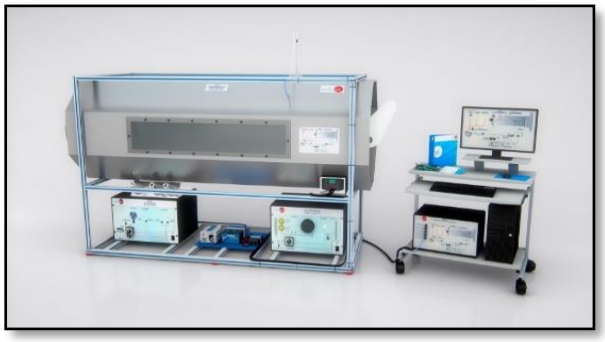

Fig. 2. Eolic Energy Unit (EEEC) [7].

C. *Design of Experiment*

Before starting the experiments, DOE has been developed to select the inputs and outputs of our project. Experiments have been performed with both load and with no load condition. In no load conditions, our variables include blade pitch angle, number of blades, and wind velocity as input, while power as output. In load conditions, we need to analyse the effect of load resistance on turbine power. In DOE, thirty-six experiments in total have been designed and power has been calculated by changing blade angles 5˚, 10˚, and 20˚, however, the number of blades configuration were 2, 3, and 6 at four different wind speeds that are 3, 6, 9 and 12 m/s. Blade angle and number of blades are taken on the right side of the DOE because their variations are the most difficult one and time taking while wind speed has been put on the rightest side because their variations are easily controllable. Table 1 and Table 2 depicts the DOE for load and no-load conditions, respectively.

TABLE I. DOE for Load and No Condition

No of experiments	Load Condition	Pitch angle	Number of Blades	Wind Speed m/s	Load resistance (%)
1, 2, 3 & 4	No Load	5	6	3, 6, 9 & 12	Nil
5, 6,7 & 8			3	3, 6, 9 & 12	
9, 10, 11 & 12			2	3, 6, 9 & 12	
13, 14, 15 & 16		10	6	3, 6, 9 & 12	
17, 18, 19 & 20			3	3, 6, 9 & 12	
21, 22, 23 & 24			2	3, 6, 9 & 12	
25, 26, 27 & 28		20	6	3, 6, 9 & 12	
29, 30, 31 & 32			3	3, 6, 9 & 12	
33, 34, 35 & 36			2	3, 6, 9 & 12	
37	Load Condition	10	2	12	100
38					75
39					50
40					25
41					10
42			3		100
43					75
44					50
45					25
46					10

D. *Mathematical Model*

For analytical calculations, BEM theory has been used. This theory is the combination of momentum theory and blade element theory. In momentum theory, power has been calculated by applying conservation of momentum, whereas in BEM blade has been divided into different sections. Power has been calculated using local forces like lift and drag forces on each section of the blade. For calculation, the flow has been considered steady, inviscid, and incompressible. From Fig. 7, it can be observed that two forces act on the blade which are lift force and drag force. The resultant force “R” is contributing to the positive power output. It can be seen

from the Fig. 7 that force per of unit blade length is in the direction of the motion.

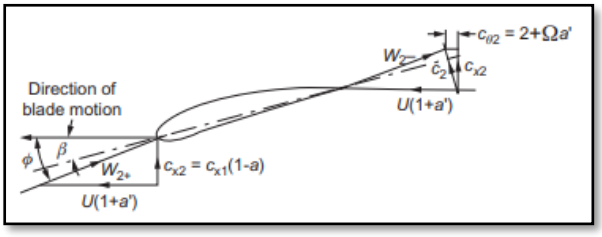

Fig. 3. Blade Element at Radius r Showing Various Velocity [9].

Resultant of relative velocity immediately upstream of the blades is

$$w = \left[{C_{x_1}}^2(1-a)^2 + (\Omega r)^2(1+a')^2\right]^{0.5}$$

$$\tan\emptyset = \frac{C_{x_2}}{\Omega r} * \frac{(1-a)}{(1+a')}$$

For blade loading coefficient

$$\lambda = ZlC_L/8\pi r$$

For flow angle

$$\tan\phi = \frac{R}{rJ}\left(\frac{1-a}{1+a'}\right)$$

Axial induction factor

$$\frac{a}{1-a} = \frac{\lambda(\cos\emptyset + \varepsilon\sin\emptyset)}{\sin^2\emptyset}$$

Tangential induction factor

$$\frac{a'}{1+a'} = \frac{\lambda(\sin\emptyset - \varepsilon\cos\emptyset)}{sin\emptyset\, cos\emptyset}$$

$$\varepsilon = \frac{C_D}{C_L}$$

Torque can be calculated by using following formula:

$$d\tau = \frac{1}{2}\rho c Zl\Omega^2 R^4[\frac{1+a'}{cos\emptyset}]^2(\frac{r}{R})^3 Clsin\emptyset\Delta(\frac{\mathrm{r}}{\mathrm{R}})$$

Generated power is:

$$d\tau = \frac{1}{2}\rho c Zl\Omega^2 R^4[\frac{1+a'}{cos\emptyset}]^2(\frac{r}{R})^3 Clsin\emptyset\Delta(\frac{\mathrm{r}}{\mathrm{R}})$$

$$P = \tau\Omega$$

Prandtl Correction Factor: BEM does not counter the effect of a finite number of blades so special correction factor has been introduced to include the finite number blades effect. As the induced velocities at any point of blades are not constant, thus it results in the reduction of net momentum and generated power of turbine. So, force can be expressed as [9]:

$$F = \left(\frac{2}{\pi}\right)\cos^{-1}\left[\exp\left(-\frac{\pi d}{s}\right)\right]$$

Here

$$\pi d/s = \frac{1}{2}Z(1-r/R)(1+J^2)^{0.5}$$

Axial and tangential induction factor becomes

$$\frac{a}{1-a} = \frac{\lambda(\cos\emptyset + \varepsilon\sin\emptyset)}{F\sin^2\emptyset}$$

$$\frac{a'}{1+a'} = \frac{\lambda(\sin\emptyset - \varepsilon\cos\emptyset)}{F\, sin\emptyset\, cos\emptyset}$$

Another correction is needed because if the value of the axial induction factor exceeds 0.3 this theory becomes invalid, so to cater this problem, formula of the axial induction factor changes if the value is greater than 0.3. Whereas it remains constant for torque and power.

$$a = \frac{1}{2}\left\{2 + K[1-2a_c] - \sqrt{[2+K(1-2a_c)]^2 + 4[Ka_c^2 - 1]}\right\}$$

$$K = \frac{4\,\mathrm{F}\sin^2\emptyset}{\sigma_\mathrm{r}(\mathrm{C_L}\cos\emptyset + \mathrm{C_D}\sin\emptyset)}$$

Fig. 4. shows the steps of the application of BEM theory, which is an iterative scheme. Here the first value of axil and tangential induction factor is assumed as zero, and the other parameters are calculated. These values have been used in the equation mentioned above, and the process has been repeated until the value of axial and tangential induction factors converges. For using BEM theory MS Excel code has been developed to calculate our desired outputs.

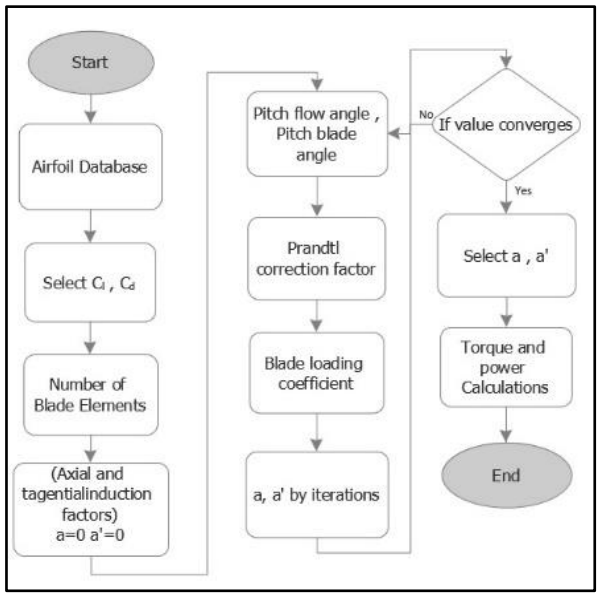

Fig. 4. Steps of BEM theory.

E. CAD Modelling

Blade modelling: A wind turbine blade is made by the combination of many aerofoil sections. The blade's cord length varies in these sections. So, the aerofoil profile for each section has been drawn for these sections by dividing the wind turbine blade into different planes. The cord length and thickness of these sections were recorded manually by using a vernier calliper at each section. The blade profile has been drawn on blank paper, and its picture has been imported into Solidworks using the sketch picture feature as shown in Fig. 5.

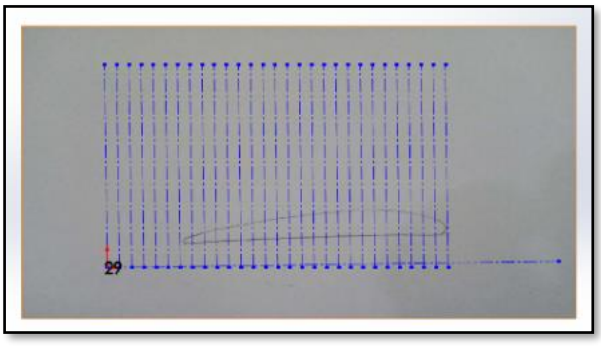

Fig. 5. Aerofoil CAD Modelling

The drawn profile has been divided into small equal sections; the spline feature has also been used to draw a two-dimensional representation of the blade aerofoil. Once the aerofoil has been profiled, its dimensions for each section including cord length and thickness have been changed according to the requirements. The corresponding aerofoils have been projected to their corresponding plane. These sections formed the skeleton of the blade; the loft option in SOLIDWORKS has been used to skin over the sections as shown in Fig.6.

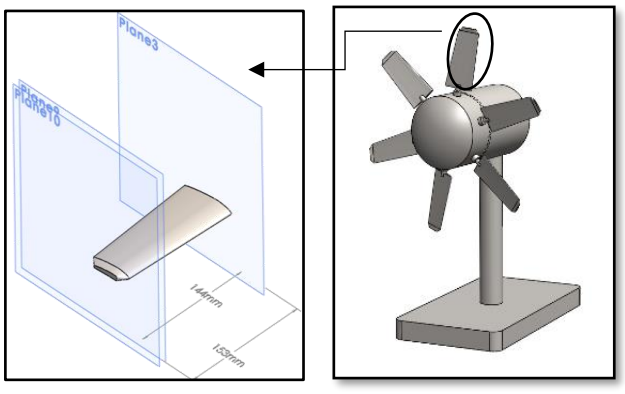

Fig 6: HAWT complete assembly in SOLIDWORKS.

CAD model assembly: The final parts of the wind turbine have been assembled in Solidworks using assembly drawing option. The final assembly of the turbine has been shown in the Fig. 6. This turbine has a hub diameter of 184 mm with a turbine diameter of 510 mm and is connected to a base by a connecting rod of 60 mm in diameter and 350 mm in height. The base has been made of a 50 mm thick plate. As the plate supports the entire weight of the turbine, it has been designed in such a way to have its center of gravity within the plate.

F. Computational Analysis

Computational Fluid Dynamics (CFD): CFD is the mathematical modelling of any physical scenario and then solved numerically using computation. Problems can be analyzed for fluid flow, dynamics, or other associated processes using the CFD software tool. For the analysis of the wind turbine, ANSYS-CFX has been utilized. All the steps involved starting from meshing, setup, and results have been computed using ANSYS-CFX. For the purpose of analysis, a simplified CAD model has also been considered for the turbine as shown in Fig. 7. For computational analysis, two domains have been created, one rotating domain which included a zone around the turbine inclusive of turbine blades and hub. This rotating domain had a diameter of 1.1 D with height kept at 0.2 D, the domain was placed right in the center of the stationary domain.

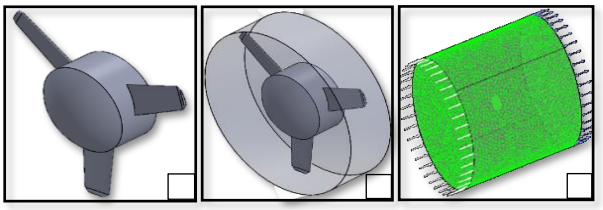

Fig. 7. Represents CAD Model and Domains for CFD Analysis (A) Simplified Model, (B) Rotary Domain and (C) Stationary Domain.

Meshing: Before CFD setup meshing has been performed. Meshing data is shown in Table II.

Table I I: Meshing Data

Meshing	Tetrahedron
No of nodes	150514
No of elements	952163
Maximum Skewness	0.93
Average orthogonal quality	0.79
Average aspect ratio	1.8
Element quality	0.84

CFD Setup: After meshing has been done on the turbine model, the mesh has been then imported into ANSYS-CFX with the boundary conditions as shown in Table III.

Table III. CFD Setup

Blade	Wind turbine blade of NACA 4309 aero foil
Flow Type	Incompressible flow
Simulation Type	Steady State
Pressure	1 atm
Pitch Angle	20˚, 10˚ and 5˚
Wind Speed	3,6,9 and 12 m/s
Turbulence Model	SST
Advanced Scheme	High Resolution
Turbulence Numeric	First Order
Wall	Scalable wall function
Boundary Conditions	• Velocity Inlet • Pressure Inlet

Pressure based solver and steady state solution have been considered for the required solution. The SST model has also been used to ensure better results for near wall and around flow separation. After the solution for the problem, which has been mostly converged around 1200 iterations, torque for each case can be displayed in postprocessor; and hence the power for each case could be calculated using the value of the computational torque and experimental RPM.

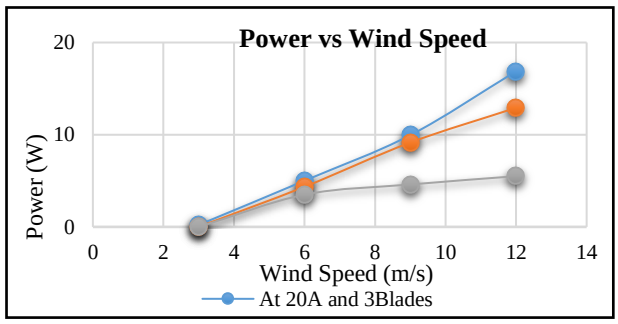

III. RESULTS

A. Experimental

The Fig. 8 shows that with the increase in wind velocity, power increases to a certain limit. Here maximum wind velocity has been limited to 12 m/s. Power increases with the increase in wind velocity because with the increase in velocity, kinetic energy also increases which causes the blade to rotate faster hence power increases. Turbine power is directly proportional to cube of wind speed. So, the power of the turbine has been greatly influenced by the variation of wind speed.

The Fig. 9 shows the relationship between the number of blades and turbine power. Here, it has been observed that an increase in the number of blades increases the turbine power. But the increase in the

Fig. 8. Relationship between Power and Wind Speed

number of blades also increases the wind resistance and cut-in speed (the speed required to start the turbine). This has been the drawback in a turbine with a larger number of blades because they only work when there is high wind velocity which is mostly unavailable.

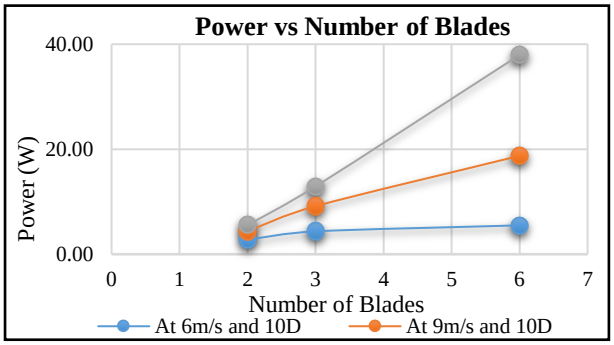

Fig. 9. Relationship between Power and Number of Blades

The Fig. 10 shows the effect of blade angle on turbine power generation. Here it has been noticed that with an increase in blade angle turbine power increases because with the increase in blade angle, lift force also increases, which causes the turbine to rotate faster and produce more power. As in the design of the experiment, we limit the blade angle to 20º. At this angle, it has been observed that power increases with an increase in blade angle, but this trend is not valid for all blade angles. Power increases to a certain limit of blade angle, after which the lift force will start decreasing, and drag force will start increasing, and eventually, turbine power will approach its minimum or zero value.

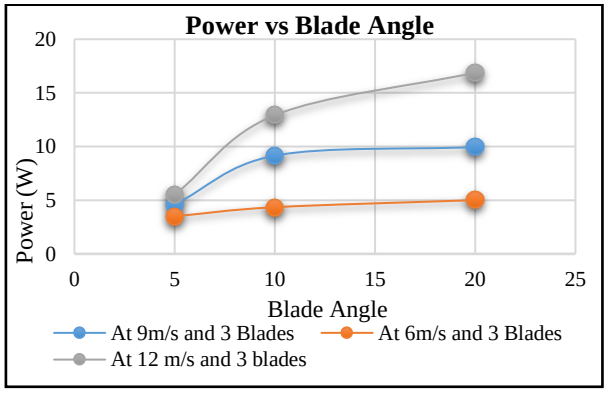

Fig. 10. Relationship between Power and Blade Angle

The Fig. 11 shows the effect of variation of load resistance on the power generation. It has been observed that with the increase in load resistance, the power generation decreases. The main aim should be to limit the generator resistance so that we can extract maximum power.

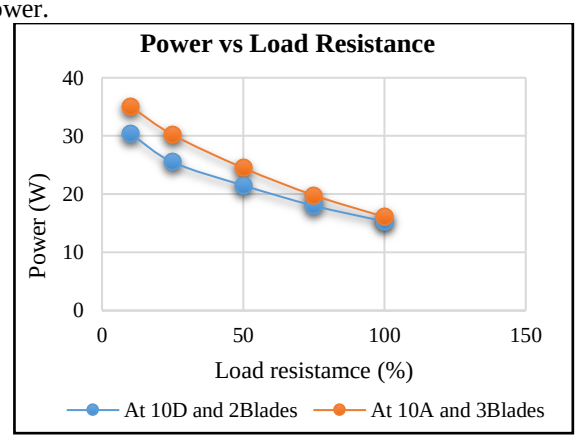

Fig. 11. Relationship between Power and Load Resistance

B. Verification & Validation

The simulations have been carried out on ANSYS CFX and results have been obtained using the ANSYS post processing menu. Simulations have been performed on all thirty-six cases but here only the results of two cases have been displayed. Results at 8 m/s with 3 number of blades and 2 number of blades have been displayed. Through computational analysis, torque has been calculated then using torque and angular velocity power generation is calculated. Fig. 12 (A) shows the pressure contours on model with velocity inlet 9 m/s, blade angle 20˚, and number of blades three. In the Fig. 12 (A) maximum pressure has a pressure with the value of 101.8 kPa has been represented by red spots and on the upper side, there has been low pressure region shown in green colour. Due to the high pressure at the lower region and low pressure at the upper region clockwise torque produces that causes the turbine to rotate in the clockwise direction. Fig. 12(B) shows the pressure contour at the YZ plane, where it can be seen that pressure is reliving at the backside of turbine. Pressure is maximum at the front side of the turbine, and it is decreased at the backside of turbine. Fig. 12(C) shows the velocity contour at the YZ plane, here it is seen that velocity is low at the backside of turbine with respect to the front side. Similarly, Fig. 12 (D) shows the pressure contours at turbine. Fig. 12 (E) show the pressure contour at the YZ plane and Fig. 12 (F) shows the velocity contour at the YZ plane.

We have calculated the computational and theoretical results for verification and validation with experimental results. All results have been verified and validated. Table IV. show the results of calculations at 20˚. Analytical power has been calculated using BEM theory, computational power has been calculated by performing simulations on ANSYS CFX and experimental power has been calculated by performing experimentations on EEEC unit present in the IC engine and power plant lab at DMAE Air University. Here maximum error between computational and experiment power has been around 19.50% and the maximum error between theoretical and computational results is 8.69%. Maximum power achieved at 20^0 blade angle using six number of blades with the wind velocity of 12 m/s has been 40 W. Maximum Coefficient of performance has been for six number of blades with the wind velocity of 9 m/s.

Table IV. Results at 20-Degree Blade Angle with No Load Condition.

Pitch angle	Number of Blades (Z)	Wind Speed (m/s)	P_{exp} (W)	P_{theo} (W)	P_{comp} (W)	Error between P_{com} and P_{exp} (%)	Error bwetween P_{theo} and P_{comp} (%)
20	6	3	0	0	0	0.00	0.00
		6	6.1	6.69	6.47	6.07	3.29
		9	20.05	21.01	21.5	7.23	2.33
		12	40.12	41.02	43.89	9.40	7.00
	3	3	0.21	0.23	0.25	19.05	8.70
		6	5.01	5.69	5.46	8.98	4.04
		9	9.95	10.27	10.73	7.84	4.48
		12	16.88	17.39	18.84	11.61	8.34
	2	3	0	0	0	0.00	0.00
		6	2.97	3.36	3.26	9.76	2.98
		9	5.59	6.21	5.99	7.16	3.54
		12	10.52	11.01	11.31	7.51	2.72

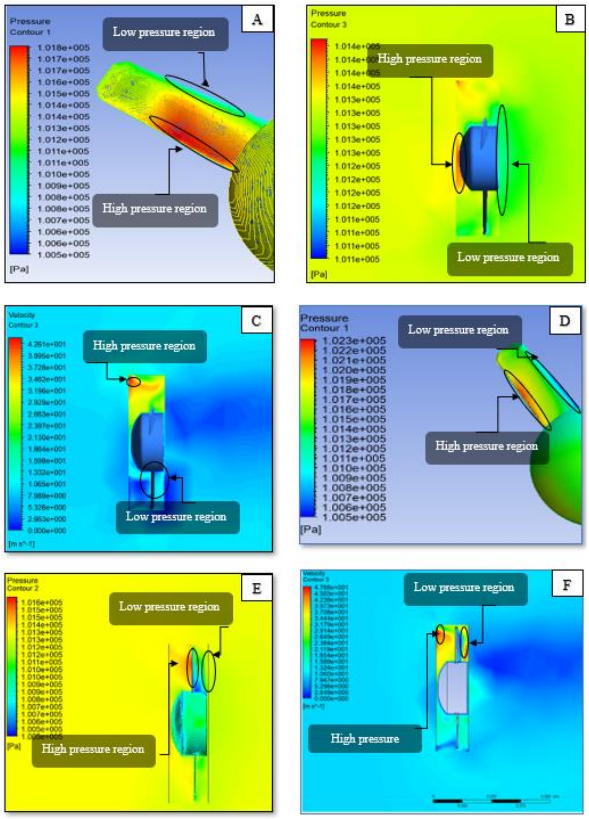

Fig. 12. Representation of Pressure Contours for (A) Blade with 9 m/s, 3 Number of Blades and 20-degree Blade Angle, (B) YZ plane with 9 m/s, 3 Number of Blades and 20-Degree Blade Angle, (C) YZ Plane with 9 m/s, 3 Number of Blades and 20-Degree Blade Angle, (D)

Table V. shows the results of calculations at 10˚ pitch angle. Analytical power has also been calculated using BEM theory, computational power has been calculated by performing simulations on ANSYS CFX and experimental power has been calculated by performing experimentations on Eolic Energy Unit (EEC) present in the IC engine and power plant lab at DMAE Air University. Here maximum error between computational and experiment power has been 8.90% and the maximum error between theoretical and computational results has been 5.83%. Maximum power achieved at 10˚ blade angle using six number of blades with wind velocity of 12 m/s has been 38 W. Maximum Coefficient of performance has been for six number of blades with the wind velocity of 9 m/s.

Table V. Results at 10-Degree Blade Angle with No Load Condition.

Pitch angle	Number of Blades(Z)	Wind Speed (m/s)	P_{exp} (W)	P_{theo} (W)	P_{comp} (W)	Error between P_{com} and P_{exp} (%)	Error between P_{theo} and P_{comp} (%)
10	6.00	3.00	0.00	0.00	0.00	0.00	0.00
		6.00	5.50	5.76	5.91	7.45	2.60
		9.00	18.74	19.37	20.50	9.39	5.83
		12.00	37.95	39.20	40.60	6.98	3.57
	3.00	3.00	0.00	0.00	0.00	0.00	0.00
		6.00	4.35	5.09	4.74	8.97	6.88
		9.00	9.15	9.69	9.82	7.32	1.34
		12.00	12.92	13.46	14.04	8.67	4.31
	2.00	3.00	0.00	0.00	0.00	0.00	0.00
		6.00	2.78	3.15	3.03	8.99	3.81
		9.00	4.41	4.61	4.78	8.39	3.69
		12.00	5.53	5.78	5.97	7.96	3.29

Table VI. show the results of calculations at 5o. Analytical power has been calculated using BEM theory, computational power is calculated by performing simulations on ANSYS CFX and experimental power has been calculated by performing experimentations on EEEC present in IC Engine and power plant lab at DMAE Air University. Here maximum error between computational and experiment power has been 32.50% and maximum error between theoretical and computational results has been 5.36%. Maximum power achieved at 5o blade angle using six number of blades with wind velocity of 12 m/s has been 5.5 W. Maximum Coefficient of performance has been for six number of blades with wind velocity 6 m/s has been 0.26.

Table VI. Results at 5-Degree Blade Angle with No Load Condition.

Pitch angle	Number of Blades (Z)	Wind Speed (m/s)	P_{exp} (W)	P_{theo} (W)	P_{comp} (W)	%Error between P_{com} and P_{exp}	%Error between P_{theo} and P_{comp}
5							
	3	3	0	0	0	0.00	0.00
		6	3.5	3.75	3.9	12.00	4.53
		9	4.6	4.98	5.2	13.04	4.42
		12	5.5	5.78	6	8.18	2.94
	2	3	0.4	0.56	0.5	32.50	5.36
		6	2.47	2.85	2.7	10.12	4.56
		9	3.08	3.31	3.4	11.69	3.93
		12	4.7	5.35	5.1	8.94	4.30

The Table VII. shows the results of experiment perform at load condition. At load conditions experiments have been performed at 10o blade angle only. Here maximum power has been achieved for three number of blades for load resistance 10% case.

Table VII. Results at Load Condition.

No of experiments	Pitch angle	Number of Blades (Z)	Load resistance (%)	Power (W)
1	10	2	100	15.3
2			75	18.01
3			50	21.5
4			25	25.5
5			10	30.4
6		3	100	16.08
7			75	19.8
8			50	24.5
9			25	30.2
10			10	35.1

IV. CONCLUSION

In the present work, analysis of small-scaled HAWT has been performed both computationally and experimentally. Analytical calculations have been executed using BEM theory, which has been critical for the verification of results. The DOE approach has been used to provide a road map for future work on this project. The turbine has been analyzed, taking pitch angles, wind speed, and the number of blades as variables. Three pitch angles (5˚, 10˚, and 20˚) with three different blade configurations (two, three, and six blades) against four wind speeds (3, 6, 9, and 12 m/s) have been considered for the present work, bringing the total

number of cases up to thirty-six for no-load condition. The CAD model corresponds to the turbine of computer-controlled wind energy unit equipment that has been developed in SOLIDWORKS. The CFD analysis and post-processing have been performed in ANSYS-CFX. The angular velocity for CFD has been provided based on experimental data. The experiments on both load and no-load conditions have been carried out in the wind tunnel. Torque, RPMs, coefficient of performance, and tip speed ratios, during experimentations, have been measured by SCADA software, which has been responsible to control wind speeds and operate the EEEC unit. It has been found that an increase in wind velocity increases the power generation of the turbine because an increase in velocity also increases the kinetic energy which causes the blade to rotate faster hence, power generation has been maximum for 12 m/s wind velocity as this has been the uppermost limit of the velocity in DOE. Power generation for 20° pitch angle has been maximum among the other blade angles in DOE. The maximum power generation has been recorded for a six-bladed case at 12 m/s wind velocity. The power generated in the said case comes out to be 40 watts. Simulation data has been compared to theoretical and experimental data to both verify and validate the results. The limitations of the project are as follows:

1. The maximum possible wind velocity in EEEC has been about 12 m/s. It means only four data points in terms of wind velocity (3, 6, 9, and 12 m/s) could be considered.
2. Experimentations on four number of blades have not been conducted due to faulty apparatus. Only three data points in terms of the numbers of blades (2, 3, and 4 blades) could be possible.
3. There is no proper marking on the DC load rheostat module, which makes it difficult to read the actual value of resistance. This creates the possibility of getting less precise results.
4. Damaged blades have been recovered; this also creates the possibility of less precise results.

V. RECOMMENDATION

Followings are the recommendations that can be considered for future work:

1. Due to faulty apparatus, experiments on four and six blades have not possible. In the future, after repairing the hub of the turbine, research should be extended to four and six blades.
2. As in this project, blade angle variation has been limited to 20˚. But in the future, blade angle variation will be extended to 90˚.
3. Experiments on load conditions has been performed only on the DC load module, in present work. Future experiments can be extended by using the AC module.
4. After some modifications, the turbine project can be extended by studying the effect of yaw angle variation on turbine performance.
5. Circulations in the wake region can be studied by using smoky or colored air.

VI. REFERENCES

[1] U. Nations, "The Sustainable Development Goals Report 2016," 2016.

[2] I. IRENA, "Future of wind: Deployment, investment, technology, grid integration and socio-economic aspects," *Abu Dhabii*, 2019.

[3] R. Rahul, S. Muralikrishnan, and T. Velayutham, "DESIGN, COMPUTATIONAL AND EXPERIMENTAL ANALYSIS OF A SMALL HORIZONTAL AXIS WIND TURBINE A PROJECT REPORT," 2012.

[4] F.-B. Hsiao, C.-J. Bai, and W.-T. Chong, "The performance test of three different horizontal axis wind turbine (HAWT) blade shapes using experimental and numerical methods," *Energies*, vol. 6, no. 6, pp. 2784-2803, 2013.

[5] M. M. Eswaran, M. Bruno, and P. E. Nicholas, "Aerodynamic Design and Analysis of Horizontal Axis Wind Turbine (HAWT) Blades Using CFD," *International Journal of Engineering Research & Technology (IJERT)*, vol. 5, no. 7, 2017.

[6] C.-J. Bai and W.-C. Wang, "Review of computational and experimental approaches to analysis of aerodynamic performance in horizontal-axis wind turbines (HAWTs)," *Renewable and Sustainable Energy Reviews*, vol. 63, pp. 506-519, 2016/09/01/ 2016, doi: https://doi.org/10.1016/j.rser.2016.05.078.

[7] Edibon, *Practical exercise manual for Eolic Energy Unit (EEEC)*. 2013, p. 92.

[8] "What is design of experiments (DOE)?," in *ASQ* vol. 2023, ed.

[9] S. L. Dixon and C. Hall, *Fluid mechanics and thermodynamics of turbomachinery*. Butterworth-Heinemann, 2013.